Eur. Phys. J. B **17**, 227–233 (2000)

THE EUROPEAN PHYSICAL JOURNAL B

EDP Sciences

Bromine metallization studied by X-ray absorption spectroscopy

A. San Miguel[1,a], H. Libotte[2], J.P. Gaspard[2], M. Gauthier[3], J.P. Itié[3], and A. Polian[3]

[1] Département de Physique des Matériaux, Université Claude Bernard-Lyon 1, 69622 Villeurbanne Cedex, France
[2] Physique de la Matière Condensée, Université de Liège, B5, 4000, Sart-Tilman, Belgique
[3] Physique des Milieux Condensés, B77, Université P. et M. Curie, 4 place Jussieu, 75352 Paris Cedex 05, France

Received 20 March 2000

Abstract. Bromine has been studied up to a pressure of 110 GPa by X-ray absorption spectroscopy (XAS) at the bromine K-edge, that allows to measure the pressure evolution of the width of the unoccupied conduction band. At 25 ± 5 GPa we observe a slope change in the evolution of this width. Comparison with published calculations of the electronic density of states indicates that the physical origin of the slope change is compatible with the metallisation process. This is also confirmed by a simple tight binding calculation. In addition, the metallisation pressure value is in agreement with calculated ones. At 68 ± 5 GPa a discontinuity in the evolution of the width of the sigma antibonding band points out the onset of a phase transformation. This result is compatible with the observed phase transformation near 80 ± 5 GPa by X-ray diffraction that is associated with the molecular dissociation.

PACS. 61.10.Ht X-ray absorption spectroscopy: EXAFS, NEXAFS, XANES, etc. – 61.50.Ks Crystallographic aspects of phase transformations; pressure effects – 61.66.Bi Elemental solids

1 Introduction

The properties of molecular solids are of central interest, both from a theoretical point of view as well as for their applications, for example in astrophysical problems. Among molecular solids, those built from diatomic molecules like I_2, Br_2 or O_2 are of special interest with respect to the metallization process. In fact, they may be used as models for the metallization of solid hydrogen which, at the present state of theoretical calculations, may happen above 300 GPa at ambient temperature and is therefore still out of reach for static compression [1]. For these reasons a great deal of effort has been devoted in the last years to improving the understanding of the non metal-metal transition in simple molecular systems, in particular in solid [2–9] and liquid [10,11] halogens (I_2, Br_2, Cl_2).

Under ambient conditions, iodine is solid with an orthorhombic structure ($D_{2h}^{18} - Cmca$) [12]. At ambient temperature, chlorine and bromine crystallize with the application of low pressure in the same orthorhombic structure. This structure is layered with the molecules lying in planes disposed perpendicular to the a axis (Fig. 1). The distance between the closest bromine atoms lying in neighboring planes is comparable with the van der Waals diameter, indicating that, at low pressure, the interaction between planes is dominated by van der Waals type potentials. On the contrary, inside the molecule planes (the bc planes), the shortest intermolecular bond is significantly shorter than the van der Waals diameter and consequently these materials cannot be considered as purely

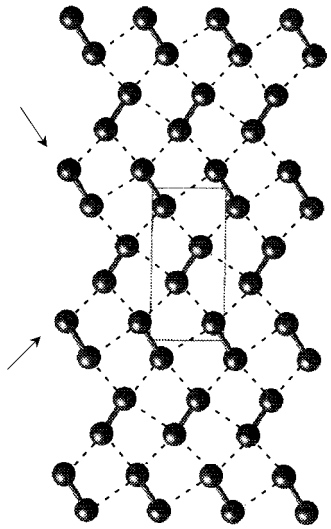

Fig. 1. Structure of one layer of the low pressure phase of solid halogens ($D_{2h}^{18} - Cmca$). The intra-molecular bonds are noted with a solid line. The two arrows point to the perpendicular directions where the Peirls type distortions are observed (see text). The unit cell is depicted. The full structure can be obtained by stacking the planes in the a direction (perpendicular to the layers) with an additional $(0, 1/2, 0)$ translation.

[a] e-mail: sanmigue@dpm.univ-lyon1.fr

molecular crystals. In fact, it has already been pointed out that in the absence of covalent intermolecular bonding, the structure of iodine should be simple cubic [13]. Nevertheless, because the intramolecular distance is much smaller than the inter-molecular ones, the low pressure phase of the halogens is referred to as a molecular crystal. The structure of the low pressure phase of solid halogens can be understood in terms of a Peierls distortion. Indeed, a partially filled p band is known to be unstable with respect to a periodic distortion, the wavelength of which depends on the number of p electrons [14,15]. For a 5/6 filled p band, if all the three directions of the space are equivalent, a distortion of the cubic cell is expected giving rise to a period of the distorted cell that is 6 times the period of the original simple cubic cell. In this paper this will be referred as a 6-merization. An alternative solution that breaks the symmetry is the layer structure of halogens, where the anisotropy gives rise to a Peierls distortion with a 4-merization in two orthogonal directions of the plane as shown in Figure 1. This opens a gap in the Fermi level.

X-ray diffraction studies show that iodine and bromine follow a first order pressure induced phase transformation towards a body-centered orthorhombic structure (D_{2h}^{25} – $Immm$). In this phase, the molecules lie in planes within which the intra and inter molecular distances are equal. To underline this fact, the formation of this 2-dimensional association has been called the monoatomic phase and the phase transformation "molecular dissociation". This has been observed to happen at 21 GPa [4,16] for iodine, near 80 GPa [8,17] for bromine, and it has been predicted to happen at 220 ± 40 GPa for chlorine [8].

Because of its lower transition pressure iodine has been extensively studied. Under ambient conditions, solid iodine is a semiconductor with an optical gap of 1.35 eV. From the detailed study of the transport and optical properties, Drickamer and co-workers [2,18] found that the onset of the metallic behavior takes place in the direction perpendicular to the layers *via* progressive gap closure and at a pressure lower than the dissociation pressure. In the layered direction the onset of a metallic behavior was also observed at a higher pressure that matches the dissociation pressure within the error bars. X-ray diffraction studies gave no evidence of structural changes associated with the onset of metallization [4,16,19,20]. The experimental results of Drickamer and co-workers are confirmed by semi-empirical tight binding calculations on the Bersohn-Rosenberg model for iodine [6]. In fact this simple model shows that the gap of the p_z band due to the weaker interaction between bc planes decreases more rapidly with pressure and closes at a lower pressure than the gap due to $p_x p_y$ orbitals inside the planes. The monoatomic iodine high pressure phase can be expected to be a "hole conductor" because of the $(4s)^2(4p)^5$ electronic configuration that provides seven valence electrons, that is to say, one hole. This is in agreement with band structure calculations in the high pressure phase [21] and is experimentally confirmed by transport measurements [22]. It is worthwhile to note that the value for the metallization pressure of iodine given by Riggleman and Drickamer [18] of 16 GPa – the value commonly found in the literature – must be corrected from the calibration of the pressure scale of the high pressure apparatus done afterwards by Drickamer [23]. This is shown in Figure 2, from where we deduce metallization pressures for iodine of 13 ± 2 GPa in the layers and 17 ± 2 GPa perpendicular to the layers. At higher pressures iodine follows a second order transformation to a body centered tetragonal phase at 43 GPa [24]. In this new phase the Peierls distortion of bc planes disappears and a planar square lattice is obtained. A first order transition to a face-centred cubic phase at 55 GPa was also reported [25] and this new phase remains stable at least up to 276 GPa [26].

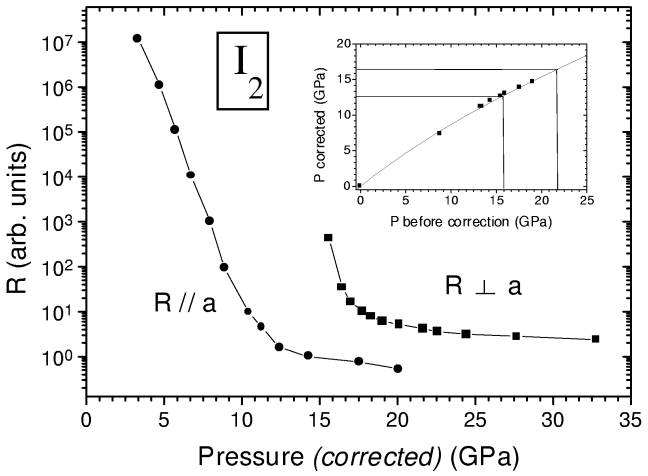

Fig. 2. Recalibration of the iodine electrical measurement of (A.S. Balchan, H.G. Drickamer, J. Chem. Phys. **34**, 1948 (1961); B.M. Riggleman, H.G. Drickamer, J. Chem, Phys. **38**, 2721 (1963)) from the pressure calibration given in (H.G. Dirckamer, Rev. Sci. Inst. **41**, 1667 (1974)). The inset shows the correspondence between the uncorrected and corrected pressure values and the correspondence between the metallization values given in the original papers (16 and 22 GPa) and the corrected ones (13 and 17 GPa).

A similar scheme of phase transformations can be expected for bromine and chlorine, but experimental or theoretical results are much scarcer than in the iodine case. We will restrict our discussion to the processes of metallization and of molecular dissociation. None of these transformations have been observed in chlorine where X-ray diffraction studies have been performed up to 45 GPa [27]. In bromine, the onset of the first order phase transformation associated with the molecular dissociation was evidenced by X-ray diffraction experiments [17] at 80 GPa. The structure refinement [8] of the low pressure phase gives the evolution of the interatomic distances with pressure. In the low pressure phase, the compression reduces the intermolecular distance whereas the intramolecular distances do not show a significant variation with pressure. At the phase transition edge (80 GPa) the difference between intra and inter molecular distances is only 8% (to be compared with 43% of difference at ambient conditions) but the equality between inter and intra

Table 1. Measured calculated and predicted transition pressures for the metallization and dissociation of solid halogens.

	P metallization (GPa)			P dissociation (GPa)	
	Exp.	Calc.	Predicted	Exp.	Predicted
Cl_2	-	$67^{\dagger}$	165^{+}	-	$220 \pm 40^{+}$
Br_2	$25 \pm 5^{*}$	$33^{\dagger}$, $35^{\S\S}$	60^{+}	$80 \pm 5^{\ddagger}$, $68 \pm 5^{*}$	$80 \pm 5^{+}$
I_2	$13 \pm 2^{\sharp}$	$15^{\dagger}$	16^{+}	$21 \pm 2^{\S}$	$21 \pm 2^{+}$

(*) This work.
(♯) Pressure calibration of the data of B.M. Riggleman, H.G. Drickamer, J. Chem. Phys. **38**, 2721 (1963) (see text for details).
(†) F. Siringo F. Piccitto, R. Pucci, High Pressure Research **3**, 162 (1990).
(+) Structural scaling rule of H. Fujihisa, Y. Fujii, K. Takemura, O. Shimomura, J. Phys. Chem. Solids **56**, 1439 (1995).
(‡) Y. Fujii, K. Hase, N. Hamaya, Y. Ohishi, A. Onodera, O. Shimomura, K. Takemura, Phys. Rev. Lett. **58**, 796 (1987).
(§) K. Takemura, S. Minomura, O. Shimomuran, Y. Fujii, Phys. Rev. Lett. **45**, 1881 (1980).
(§§) H. Miyagi, K. Yamguchi, H. Matsuo, K. Mukose, J. Phys. Condens. Matter **10**, 11203 (1998).

molecular distances only takes place in the high pressure phase after a volume reduction, $\Delta V/V$, of 3% at the phase transformation.

Our work was motivated by the lack of experimental data concerning the metallization process of bromine and in particular the value of the metallization pressure. In addition some predictions for the metallization pressure of bromine and chlorine [6,8,9] are in serious contradiction (see Tab. 1) giving values that differ by a factor two for bromine and even more for chlorine. In order to obtain a more complete description of the high pressure behavior of solid bromine we have performed X-ray absorption spectroscopy experiments at the Br K-edge up to a pressure of 110 GPa. X-ray absorption spectroscopy (XAS) [28] is a very powerful technique to explore local properties of matter. Information of the local structure and electronic structure can be obtained from the spectra. In the case of bromine, there is a very prominent peak feature just before of the jump of the bromine K-edge. This feature was extensively studied in the early days of EXAFS (Extended X-ray Absorption Fine Structure) and it was shown [29] through the angular dependence of the spectra taken on a bromine-on-graphite system, that this peak is due to electronic transition from the $1s$ electrons to unfilled $4p$ states associated with the σ-antibonding orbitals (σ^*). In the following we will refer to that peak as the $1s \rightarrow 4\sigma^*$ transition. Because of dipolar selection rules, the structures at the beginning of the bromine K-edge X-ray absorption spectra are the projection of the p-density of free states modified by the presence of the $1s$ core-hole. In bromine, the energy modification of the ground state by the creation of one hole in the $1s$ level has been evaluated to be 7.3 eV [30]. In the case of the bromine K-edge no quadrupolar contributions should be expected. Similarly to solid bromine there exists an important covalent coupling between bromine molecules giving rise to a $1s \rightarrow 4\sigma^*$ feature in the electronic spectrum corresponding to the transitions to the very narrow conduction band of solid bromine. The evolution of the electronic structure of bromine with density will be reflected in the features of the $1s \rightarrow 4\sigma^*$ peak and can be used as a fingerprint of phase transitions or electronic changes. It would also have been of major interest to follow the EXAFS signal with pressure. Unfortunately, as explained below, this was not accessible in this experiment.

2 Experimental

X-ray absorption spectra were taken at the energy dispersive XAS beamline (ID24) of the ESRF (European Synchrotron Radiation Facility). A specially profiled Bragg Si (111) crystal polychromator [31,32] was used in order to disperse the undulator white-beam around the Bromine K-edge energy (13.474 keV). Harmonic rejection was ensured by the double reflection of the white beam on the Kirkpatrick-Baez optics placed before the polychromator. The reflected beam by the polychromator was focussed on to the sample in the horizontal plane to approximately 150 μm and further slitted by the sample environment to 30 μm. In the vertical plane the beam was defined by slits to 50 μm. Due to of the very high pressure that was required, high focusing was an essential parameter in this experiment. The ID24 spectrometer allows focusing of 50 μm of the polychromatic beam for energies between 5 and 11 keV, but this value rapidly increases when going to higher energies due to the X-ray penetration in the curved polychromator crystal. More details concerning the ID24 spectrometer can be found elsewhere [33]. Pressure was generated using a membrane diamond anvil cell with a large angular aperture [34] in which bevelled diamonds with 100 μm diameter culets were mounted. Liquid bromine was introduced in to the hole of 30 μm diameter drilled in a rhenium gasket. The pressure transmitting media was the sample itself. Pressure was measured in situ through the luminescence of a ruby chip introduced with the sample [35] and special care was observed to avoid hydration of the sample during the loading process [36]. The loading was performed in a glove box under inert atmosphere. The intensity of the pre-edge feature of the XAS spectra was used to determine any possible chemical degradation of bromine. In fact, we have observed that when bromine has been exposed to air the intensity of the pre-edge feature decreases to more than half when compared to a pure sample. The diamond anvil cell was oriented with respect to the X-ray beam in order to avoid the presence of diamond diffraction glitches in the zone of interest around the absorption edge. The main experimental problem arises when reducing the size of the beam in the vertical direction by slitting. In fact, when the vertical dimension was less than 100 μm, very sharp structures in the X-ray beam appear in the signal. These structures are of the same magnitude as the signal of the EXAFS oscillations at 50 μm of slit size. Nevertheless, the intensity of the pre-edge feature is more than 10 times the amplitude

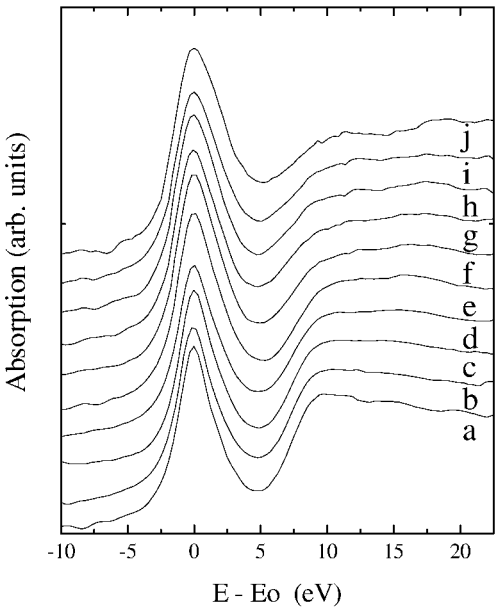

Fig. 3. Edge region of the X-ray absorption spectra of bromine at the K-edge as a function of pressure. The spectra have been shifted in the vertical direction for clarity. Labels correspond to the sample pressure : a (8.1 GPa), b (9.5 GPa), c (13.2 GPa), d (17.8 GPa), e (24.8 GPa), f (41 GPa), g (63 GPa), h (65 GPa), i (71 GPa), j (110 GPa). The energy origin has been arbitrarily fixed at the maximum of the pre-edge feature.

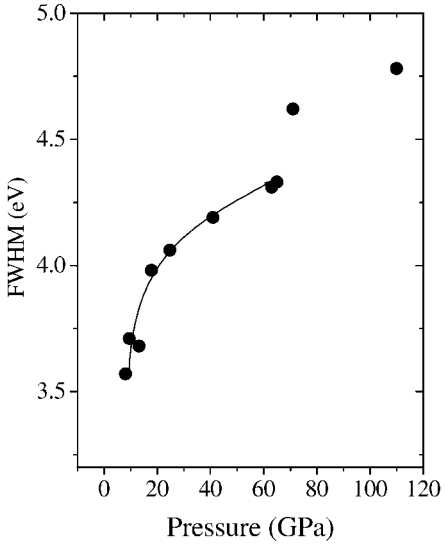

Fig. 4. Observed full-width-half-maximum of the evolution with pressure of the pre-edge peak ($1s \rightarrow 4\sigma^*$ band transition) as a function of pressure.

of the EXAFS oscillations and, being only slightly affected by the presence of these structures, it can be exploited. The origin of the spurious structures that appear at low vertical slitting is the strong coherence of the X-ray beam related to the small emittance of the ESRF electron beam. However, without this small emittance, it would have been difficult to attain the reduced horizontal beam size needed for the experiment. For each bromine spectra, a reference spectrum of KBr at the Br K-edge was taken in order to make the energy calibration by comparing with a spectrum obtained with a two crystal monochromator [37].

3 Results

In Figure 3 we show the edge region of the X-ray absorption spectra as a function of pressure. The energy origin was arbitrarily set at the maximum of the pre-edge feature. In our first spectrum taken at 8.1 GPa, we observe a difference between the 1s and the continuum energy levels, $\Delta E = E_{1s\rightarrow\infty} - E_{1s\rightarrow\sigma^*}$ of 7.3±0.5 eV a value that is in good agreement with other measured [38] and calculated [30] values (8 eV). We have taken as value for the $1s \rightarrow 4\sigma^*$ transition the maximum of the pre-edge feature and for the $1s \rightarrow \infty$ one, the value of the inflexion point at the edge. No clear trend was observed in the evolution of ΔE with pressure that seems to be constant within our sensitivity. This means that the relative position between the bottom of the conduction band and the continuum level (the minimum energy need to consider a photoelectron as a free propagating wave) is constant within this limit. This is in good agreement with band structure calculations performed on the low pressure phase of iodine [6,9]. It is possible to fit the pre-edge feature with a single Lorentzian function. We nevertheless observe a progressive (linear) degradation of this fitting when the pressure is applied to the sample. A fit with two Gaussian functions gives a good representation of the pre-edge feature for all pressures. In that case, the higher energy peak contribution to the pre-edge increases linearly with pressure going from 14% of the total area at the lowest pressure measured (8.1 GPa) up to 25% at 71 GPa. At 1.2 Mbar, both peaks contribute in a similar way to the total signal. This trend is also observed in the calculated density of states within the full-potential linear muffin-tin orbital method (FPLMTO) [9]. The pressure evolution of the FWHM of the pre-edge feature is a measure of the evolution of the width of the $4\sigma^*$ empty band. The measured evolution of this FWHM with respect to pressure is shown in Figure 4. It has been observed, for all the pressure domain explored, that a positive slope of the curve as is expected for a progressive augmentation of density. It is also obvious that up to 25 ± 5 GPa this slope is greater than that between 25 ± 5 and 63 ± 5 GPa. In addition, a clear discontinuity is observed in the evolution of the FWHM of the $1s \rightarrow 4\sigma^*$ feature at 68 ± 5 GPa. Such a discontinuity can only be related to a discontinuous change of the evolution of the electronic structure of bromine. The pressure at which it is observed, 68 ± 5 GPa, is slightly lower than the observed phase transformation pressure (80 ± 5 GPa) associated with the molecular dissociation [8,17]. It is closer to the metallization pressure for bromine (60 GPa) obtained from scaling rules [8]. Unfortunately there is a lack of experimental data that could allow to check if there is or not a further change – corresponding to the structural phase transformation – at 80 GPa. Nevertheless, all calculations and observations

show that the gap closure of iodine is progressive and without discontinuity and we expect the same trend for bromine. In that case, the observed discontinuity could only be associated to the molecular dissociation. The difference between our value for the dissociation pressure and the published one [8,17] can have different origins: i) an underestimation of the error bars (we recall here that bromine itself is serving as pressure transmission medium) ii) the different sensitivity to the phase transition of a local probe (X-ray absorption spectroscopy) and of a long range-order probe (X-ray diffraction). The experimental problems already reported prevent us from extracting quantitative structural information from the EXAFS or the XANES (X-ray Absorption Near Edge Structure) parts of the spectra. Nevertheless, it can be observed from Figure 3 that the XANES part (the region situated after the edge in the figure) progressively changes with pressure. This is an indication of an evolution of the local structure around the bromine atom related to the density reduction. Better data quality is needed for the extraction of quantitative information from this part of the spectra.

4 Model description

In order to obtain a physical explanation of the slope change of the FWHM of the XAS pre-edge feature that is observed at 25 ± 5 GPa, a semi-empirical tight-binding model is used.

The Fermi energy, E_{F} is defined by

$$N_{\mathrm{el}} = \int_{-\infty}^{E_{\mathrm{F}}} n_p(E)\mathrm{d}E \tag{1}$$

where $n_p(E)$ is the electronic density of states and N_{el} is the number of p electrons per atom (in the case of bromine, $N_{\mathrm{el}} = 5$). In a first approximation, the $4s$ levels are filled and therefore, they do not contribute to the band energy.

Our model description is based on a simplification of the real crystallographic structure. In a first approximation, the two directions in the molecular layers (the 4-merised direction shown by arrows in Fig. 1) are assumed to be independent. This is exact if the angles are equal to 90° and if only the $pp\sigma$-orbital interactions, which are the most important interatomic interactions, are taken into account ($pp\pi = 0$). Therefore, the electronic density of states is calculated for a 1-D chain of bromine atoms linked to their neighbours by one short bond (intramolecular) and three long bonds. In the z-direction, a simple linear chain of atoms linked by long bonds is considered.

Under these assumptions the tight-binding Hamiltonian writes

$$H_{\mathrm{el}}^{1D} = \sum_i \epsilon_p |\phi_i\rangle\langle\phi_i| + \sum_i \sum_{j\neq i} \beta_{pp\sigma}^{ij} |\phi_i\rangle\langle\phi_j| \tag{2}$$

where $|\phi_i\rangle$ is the p atomic orbital located on site i, ϵ_p is the p electronic level and $\beta_{pp\sigma}^{ij}$ is the resonance integral between $|\phi_i\rangle$ and $|\phi_j\rangle$.

The interatomic interactions are assumed to be non-vanishing for nearest neighbours only. In addition the atomic wave functions are supposed to be orthogonal, *i.e.* $\langle\phi_i|\phi_j\rangle = \delta_{ij}$ where δ is the Kronecker symbol.

The resonance integrals, $\beta_{pp\sigma}(r_{ij})$, between neighboring atoms i and j distant of r_{ij} are assumed to have the form proposed by Slater and Koster [39]. In addition we assume a distance dependence given by relation (3) where $q = 2$.

$$\beta_{pp\sigma}(r_{ij}) = \beta_{pp\sigma,0} \left(\frac{r_{ij}}{r_0}\right)^{-q}. \tag{3}$$

If the long bonds were of infinite length a three peak electronic spectrum would appear. Long bonds of finite length would give rise to three bands, the width of each one being equal to $2\beta_{pp\sigma}(r_L)$, with r_L the long bond length.

In order to evaluate the evolution of the conduction bandwidth as a function of pressure the interatomic distances have been taken from the experimental X-ray diffraction data [8]. The electronic parameters are chosen so as to reproduce the zero-pressure optical gap calculated by Siringo *et al.* [6]. The metallization pressure is found to be at about 50 GPa. The metallization occurs when the bottom of the antibonding σ^* conduction band crosses the top of valence p_z-band. This was already found in a more detailed calculation [6] and justifies our simple approach. Figure 5 shows the calculated width of the conduction band, $W(P)$, as a function of pressure as it should be observed by XAS. It is clear that the slope of the curve changes at the metallization pressure, P_{M}. This can be explained as follow.

Below P_{M}, *i.e.* before the band crossing, the conduction band width is simply the difference between the top and the bottom of the empty conduction band. Above P_{M}, *i.e.* after metallization has occurred, the situation is different: there is an overlap between the σ^* conduction band and the p_z-band. Therefore, the observed width of the conduction band is now the difference between the top of the σ^* conduction band and the Fermi level. This is shown in the schematic representation of the band structure of Figure 5.

5 Discussion and conclusions

Our model shows that the conduction bandwidth, as observed by XAS, has a slope discontinuity at a pressure at which the metallization occurs. Experimentally, the expected presence of pressure gradients and the effect of non-zero temperature produce a continuous change of the slope and this is precisely what it is observed experimentally at 25 ± 5 GPa. This value is in very good agreement with the calculated metallization pressure [7,9] and consequently does not agree with the one deduced from structural scaling rules (see Tab. 1). As the metallization process involves the inter-plane electronic interaction, it can

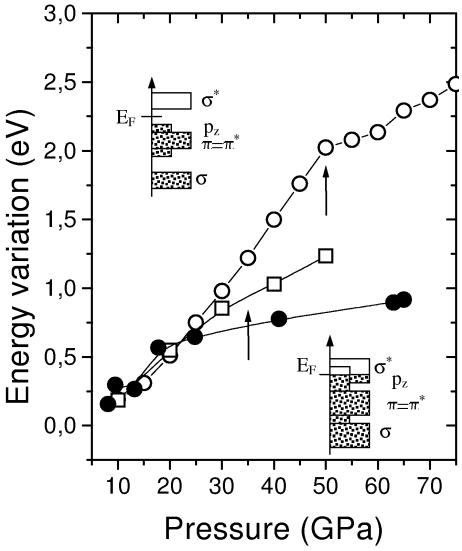

Fig. 5. Calculated (hollow symbols) and measured (filled symbols) FWHM evolution with pressure of the pre-edge peak ($1s \rightarrow 4\sigma^*$ band transition). Empty circles: within a simple tight binding calculation with the metallization pressure, P_M, that was arbitrarily set at 50 GPa (see text). Empty squares: from the electronic-DOS calculated in a full-potential linear muffin-tin orbital method and convoluted by a 0.4 eV Lorentzian function. In this case the gap closure was observed at 35 GPa. The arrow points to the metallization pressure, P_M, in the two cases corresponding to the introduction of the Fermi level in the $4\sigma^*$ band. Lines are only guides for the eye. For both calculations, the slope change corresponds to the metallization process. There are also shown the scheme of the electronic band structure before (top) and after (bottom) the metallisation.

be expected that the structural scaling rules that work remarkably well in the case of the dissociation process are not directly applicable to the metallization as it has been proposed [8]. In the same way, the electronic-DOS calculated by FPLMTO [9] also shows the same type of pressure non linear behaviour of the band-width of the σ^* conduction band from the metallization pressure (Fig. 5). In our simple model we have set arbitrarily the metallization pressure at a value of 50 GPa that is 15 GPa higher than in the FPLMTO calculation [9] and we have nevertheless obtained the slope change associated to the metallization process using the same structural data at the chosen metallization pressure. This confirms that within this model the slope change is well associated to electronic changes and not to the evolution of the compressibility of bromine. The absolute value of the band-width is difficult to compare with our experimental values that are affected by the core-hole width, the experimental resolution and pressure gradients.

It is worth to note that, in liquid iodine, a two step metallization process is observed [10] at a much lower pressure than for the solid phase (between 3 and 5 GPa). This reduced metallization pressure value indicates that an important loss of the lamellar character of the solid phase can be concluded, but at the same time, the persistence of a two step process in the liquid phase could indicate that the lamellar structure has not been totally destroyed. In other words, the Peierls distortion should then still be present in the liquid phase. This is in fact also observed in liquid elements like arsenic [40] and demonstrated theoretically. Indeed the Peierls distortion is a local effect [15] more than a long range effect. In addition, EXAFS measurements [11] show that the iodine intra-molecular distance increases slightly with pressure both in the solid and in the liquid phase, but much more rapidly for the last one. A simple tight binding computation of a Peierls distorted system shows a slight increase of the intra-molecular distance close to the dissociation pressure [41]. Consequently, the EXAFS results are also compatible with a persistence of the Peierls distortion in the liquid phase of the halogens, but significantly reduced with respect to the one of the solid phase at ambient conditions.

In conclusion, our X-ray absorption experiment shows that at 25 ± 5 GPa there is a slope change in the XAS FWHM of the pre-edge feature at the Br K-edge that can be interpreted as an evidence of the onset of the metallization process. A simple tight binding model allows us to assign the physical origin of this slope change in agreement with FPLMTO calculations [9]. The excellent agreement between the observed pressure value of 25 ± 5 GPa with the one calculated by Siringo *et al.* [7] and Miyagi *et al.* [9] reinforces the metallization assumption. Nevertheless this can not be considered as a complete proof of the metallization process because we can not give a proof of uniqueness of origin for the slope change of the FWHM and further measurements or calculations will be needed in order to verify our observation. At 68 ± 5 GPa a discontinuity in the evolution of the width of the empty conduction band points out the presence of a structural phase transformation. This transformation takes place at a pressure that is compatible with the observed phase transformation near 80 ± 5 GPa and that is associated with the molecular dissociation. In addition, we note that, to our knowledge, we have reached the highest pressure ever reported in a XAS experiment.

We are grateful to Prof. H. Miyagi (Osaka University) for providing us with the electronic-DOS files of his calculations [9].

References

1. K.A. Johnson, N.W. Ashcroft, Nature **403**, 632 (2000).
2. A.S. Balchan, H.G. Drickamer, J. Chem. Phys. **34**, 1948 (1961).
3. K. Syassen, K. Takemura, H. Tups, A. Otto, *Physics of solids under high pressure*, edited by J.S. Schilling, R.N. Shelton (North Holland Publishing Company, 1981), p. 125.
4. K. Takemura, Y. Fujii, S. Minomura, O. Shimomura, J.D. Axe, Phys. Rev. B **26**, 998 (1982).
5. M. Pasternak, J.N. Farrell, R.D. Taylor, Phys. Rev. Lett. **58**, 575 (1987).

6. F. Siringo, R. Pucci, N.H. March, Phys. Rev. B **37**, 2491 (1988); *ibid.* **38**, 9567 (1988).
7. F. Siringo, F. Piccitto, R. Pucci, High Pressure Research **3**, 162 (1990).
8. H. Fujihisa, Y. Fujii, K. Takemura, O. Shimomura, J. Phys. Chem. Solids **56**, 1439 (1995).
9. H. Miyagi, K. Yamguchi, H. Matsuo, K. Mukose, J. Phys Cond. Matter **10**, 11203 (1998).
10. V.V. Brazhkin, S.V. Popova, R.N. Voloshin, A.G. Umnov, High Pressure Research **6**, 363 (1992).
11. U. Buontempo, A. Filipponi, D. Martínez-García, P. Postorino, M. Mezouar, J.P. Itié, Phys. Rev. Lett. **80**, 1912 (1998).
12. F. van Bolhuis, P.B. Koster, T. Migechelsen, Acta Crystallog. **23**, 90 (1967).
13. K. Yamasaki, J. Phys. Soc. Jpn **17**, 1262 (1962).
14. J.-P. Gaspard, R. Céolin. Solid State Comm. **84**, 839 (1992).
15. J.-P. Gaspard, A. Pellegatti, F. Marinelli, C. Bichara, Phil. Mag. **77**, 727 (1998).
16. K. Takemura, S. Minomura, O. Shimomuran, Y. Fujii, Phys. Rev. Lett. **45**, 1881 (1980).
17. Y. Fujii, K. Hase, Y. Ohishi, H. Fujihisa, N. Hamaya, K. Takemura, O. Shimomura, T. Kikegawa, Y. Amemiya, T. Matshshita, Phys. Rev. Lett. **63**, 536 (1989).
18. B.M. Riggleman, H.G. Drickamer, J. Chem, Phys. **38**, 2721 (1963).
19. O. Shimomura, K. Takemura, Y. Fuji, S. Minomura, M. Mori, Y. Noda, Y. Yamada, Phys. Rev. B **18**, 715 (1978).
20. K. Takemura, Y. Fuji, S. Minomura, O. Shimomura, Solid State Comm. **30**, 131 (1979).
21. Y. Natsume, T. Suzuki, Solid State Comm. **44**, 1105 (1982).
22. T. Yamauchi, K. Shimizu, N. Takeshita, M. Ishizuka, K. Amaya, S. Endo, J. Phys. Soc. Jpn **63**, 2307 (1994).
23. H.G. Drickamer, Rev. Sci. Inst. **41**, 1667 (1974).
24. Y. Fujii, K. Hase, Y. Ohishi, N. Hamaya, A. Onodera, Solid State Comm. **59**, 85 (1986).
25. Y. Fujii, K. Hase, N. Hamaya, Y. Ohishi, A. Onodera, O. Shimomura, K. Takemura, Phys. Rev. Lett. **58**, 796 (1987).
26. R. Reichlin, A.K. McMahan, M. Ross, S. Martin, J. Hu, R.J. Hemley, J.K. Mao, Y. Wu, Phys. Rev. B **49**, 3725 (1994).
27. E.-Fr. Düsing, W.A. Grosshans, W.B. Holpzapfel, J. Phys. Colloq. France **45**, C8-203 (1984).
28. *X-ray Absorption*, edited by D.C. Konigsberger, R. Prins (Wiley, New York, 1988).
29. S.M. Heald, E.A. Stern, Phys. Rev. B **17**, 4069 (1978).
30. S.H. Chou, J.J. Rehr, A. Stern, E.R. Davidson, Phys. Rev. B **35**, 2604 (1987).
31. J. Pellicer-Porres, A. San Miguel, A. Fontaine, J. Synchrotron Radiation **5**, 1250 (1998).
32. A. San Miguel, M. Hagelstein, J. Borrel, G. Marot, M. Renier, J. Synchrotron Radiation **5**, 1396 (1998).
33. M. Hagelstein, A. San Miguel, A. Fontaine, J. Goulon, J. Phys. IV France **7**, C2-303 (1997).
34. J.C. Chervin, B. Canny, J.M. Besson, Ph. Pruzan, Rev. Sci. Instrum. **66**, 2595 (1995).
35. G. Piermanrini, S. Block, J.D. Barnett, R.A. Forman, J. App. Phys. **46**, 2774 (1975).
36. This problem is particularly relevant in the paper: J.P. Itié, M. Jean-Louis, E. Dartyge, A. Fontaine, A. Jucha, J. Phys. Colloq. France **47**, C8-897 (1986).
37. The reference spectrum was kindly provided by Pr. T. Murata (Kyoto University of Education).
38. T.A. Tyson, K.O. Hodgson, C.R. Natoli, M. Benfato, Phys. Rev. B **46**, 5997 (1992).
39. J.C. Slater, G.F. Koster, Phys. Rev. **94**, 1498 (1954).
40. R. Bellissent, C. Bergman, R. Céolin, J.-P. Gaspard, Phys. Rev. Lett. **59**, 661 (1987).
41. J.-P. Gaspard, private communication.